Pertanika J. Trop. Agric. Sci. 49 (S1): 171 - 192 (2026)

TROPICAL AGRICULTURAL SCIENCE

Journal homepage: http://www.pertanika.upm.edu.my/

Physical Properties and Mass Modelling of Matoa Fruit (*Pometia pinnata*) at Different Varieties

Mohd Hafizz Wondi[1]*, Nur Izzah Nabilah Haris[2], Maimunah Mohd Ali[3], Sharifah Raina Manaf[1], Abdul Rahman Saili[4], Akmal Shafiq Badarul Azam[5], Bernard Maringgal[6], Muhammad Hazwan Hamzah[7], and Muhammad Shahimi Ariffin[5]

[1]*Faculty of Plantation and Agrotechnology, Universiti Teknologi MARA Sarawak Branch, 96400 UiTM Mukah, Sarawak, Malaysia*
[2]*Department of Chemical and Environmental Engineering, Faculty of Engineering, University Putra Malaysia, 43400 UPM Serdang, Selangor, Malaysia*
[3]*Department of Food Sciences, Faculty of Science and Technology, Universiti Kebangsaan Malaysia, 43600 UKM Bangi, Selangor, Malaysia*
[4]*Faculty of Plantation and Agrotechnology, Universiti Teknologi MARA Cawangan Sarawak, 94300 UiTM Kota Samarahan, Sarawak, Malaysia*
[5]*Center of Mathematical Sciences, Faculty of Computer and Mathematical Sciences, Universiti Teknologi MARA Sarawak Branch, 96400 UiTM Mukah, Sarawak, Malaysia*
[6]*Faculty of Resource Science and Technology, Universiti Malaysia Sarawak, 94300 UNIMAS Kota Samarahan, Sarawak, Malaysia*
[7]*Department of Biological and Agricultural Engineering, Faculty of Engineering, Universiti Putra Malaysia, 43400 UPM Serdang, Selangor, Malaysia*

ABSTRACT

Matoa fruit is a tropical fruit with a native background of Southeast Asia that is very promising in terms of specific flavour and nutrient properties, yet is under a poor usage by the groups because of the lack of post-harvest studies. There are two types of mass modelling discussed in this paper to facilitate post-harvest handling, sorting, and grading: purple and red Matoa. The average mass, primary diameter, Surface Area (SA), and sphericity of purple Matoa were 42.86 g, 54.22 mm, 7133 mm², and 0.85, in comparison to 17.55 g, 40.95 mm, 3610 mm², and 0.78 of red Matoa, respectively. It is worth noting that the dimensions, SA, and volume have been used as independent parameters to come up with regression models. The quadratic model proved to have the best predictive potential. The most suitable predictor of mass was the equivalent mean diameter (D_e) with a R^2 = 0.962 and

ARTICLE INFO

Article history:
Received: 19 July 2025
Accepted: 12 December 2025
Published: 19 March 2026

DOI: https://doi.org/10.47836/pjtas.49.S1.08

E-mail addresses:
mohdhafizz@uitm.edu.my (Mohd Hafizz Wondi)
izzahnabilah@upm.edu.my (Nur Izzah Nabilah Haris)
maimunahmma@ukm.edu.my (Maimunah Mohd Ali)
sharifahraina@uitm.edu.my (Sharifah Raina Manaf)
arsaili@uitm.edu.my (Abdul Rahman Saili)
akmalshafiq@uitm.edu.my (Akmal Shafiq Badarul Azam)
mbernard@unimas.my (Bernard Maringgal)
hazwanhamzah@upm.edu.my (Muhammad Hazwan Hamzah)
mshahimi@uitm.edu.my (Muhammad Shahimi Ariffin)
* Corresponding author

e-ISSN: 2231-8542
© Universiti Putra Malaysia Press

Standard Error of Estimate (SEE) = 0.689. In line with this, the quadratic model was very good in explaining the case of SA, where $R^2 = 0.960$ and SEE = 0.714. Likewise, the model of the volume of an ellipsoid had a high predictive accuracy ($R^2 = 0.960$, SEE = 0.709). The results indicate that quadratic models are reliable in forecasting the mass of Matoa fruit, which can be used to design effective automated grading systems. This research would help to commercialise Matoa fruit in a sustainable way by removing the labour-intensive operations and increasing the value of the fruit in commercial and industrial use. Future research may focus on scalability and integration with machine vision systems.

Keywords: Mass modelling, mass prediction model, Matoa fruit, physical properties, post-harvest

INTRODUCTION

Matoa fruit (*Pometia pinnata Forst & Forst)* is a tropical tree species indigenous to the Southeast Asian region, with native populations and wide distribution across Borneo, Sumatra, and Papua New Guinea. *Pometia pinnata* trees typically reach heights of 12 to 20 metres and produce fruit that matures approximately 10 weeks after anthesis (Figure 1). The fruit is generally to in diametre and exhibits high morphological variability, occurring in several varieties distinguished by pericarp colour, such as purple, brown, yellow, red, and green. Its distinct flavour, reminiscent of longan, rambutan, and durian, has gained popularity beyond its native areas, particularly in Malaysia, where its nutritional and culinary values are increasingly acknowledged.

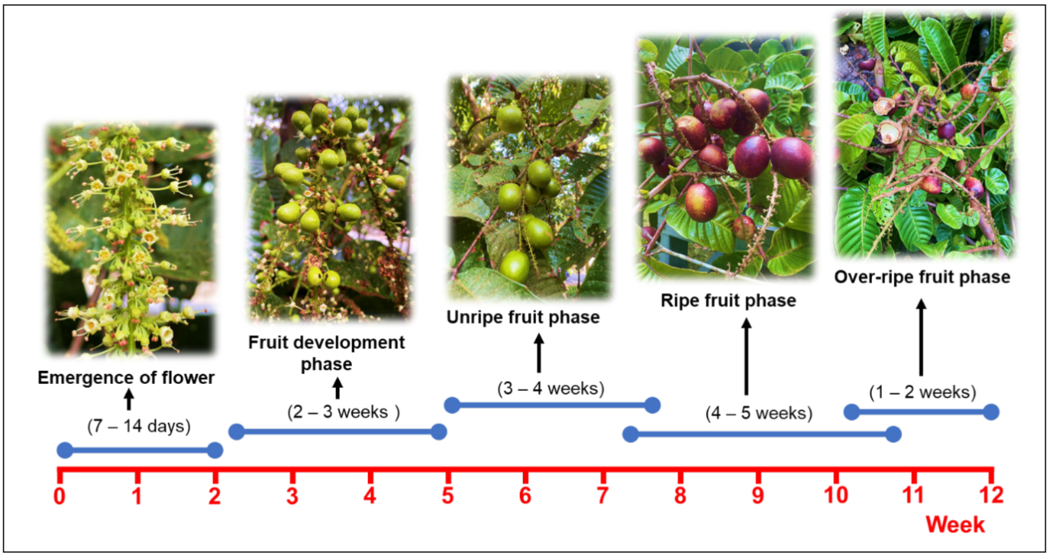

Figure 1. Timeline of Matoa fruit maturation process

Matoa fruit is rich in provitamin A carotenoids, particularly beta-carotene, which the human body metabolises into active vitamin A. Vitamin A is a powerful antioxidant, protecting cells from oxidative stress and slowing ageing. In the same manner, vitamin E enhances the circulation of the blood, thus making sure the oxygen and nutrients circulate well all over the body. Mataoa fruit has been associated with improved cardiovascular health and has been a target among health-conscious consumers when it is consumed frequently. Moreover, Matoa fruit also has bioactive substances, such as saponins, which have an antifungal, antibacterial, and larvicidal effect (Chapagain et al., 2008; Faustina & Santoso, 2017; Ghazzawi et al., 2023; Jomova et al., 2023; Mohammad et al., 2012; Sauriasari et al., 2017; Sholiha et al., 2024; Wahedi et al., 2024; Warraich et al., 2020; Wondi et al., 2025). These positive characteristics underline that it can be applied in agriculture and in the pharmaceutical industry. Nevertheless, the potential of the fruit is not fully exploited because few studies have been conducted on post-harvest processing and handling technologies.

As the popularity of Matoa fruit increases, it is important to conduct research on its physical characteristics to improve post-harvest management and realise its commercial potential. The main physical traits like colour, porosity, sphericity, aspect ratio, dimensions and mass are vital in coming up with effective packaging, grading, sorting, washing and transportation systems (Bhushan et al., 2022; Chandegara & Varshney, 2014; Lorestani et al., 2012; Mahawar et al., 2019; Wondi et al., 2024). Uniformity of size and shape is important in ensuring that automated grading and sorting systems are developed based on homogeneous physical features in order to maximise efficiency (Ahemen & Raji, 2017; Viana de Araujo et al., 2020). Hence, mass-based grading systems have become integral to post-harvest management due to their cost-effectiveness and efficiency, especially for fruits with irregular shapes. Accurate mass grading is effective to improve packaging configurations, decrease the expenses of transportation, and increase storage factors due to the assurance of uniformity (Mahawar et al., 2019; Wondi et al., 2023). Thus, it is necessary to learn the correlations between the physical properties of Matoa fruit and the distribution of its mass in order to design effective post-harvest systems that will minimise losses and maximise the market value.

Previous studies have successfully applied mass prediction models referring to the physical characteristics of various fruits, including strawberries (Birania et al., 2022), Sohiong (Vivek et al., 2018), oil palm fruitlets (Sanganamoni et al., 2024; Wondi et al., 2021), *Terminalia chebula* (Sumit Sudhir et al., 2019); pepper berries (Megat Ahmad Azman et al., 2020), dabai (Afiqah et al., 2024), wood apple (Grover et al., 2024; Murakonda et al., 2022), coconut (Pandiselvam et al., 2019), and banana (Kamble et al., 2021). Although similar research has been successful on other fruits, no published research can be found to determine the physical properties and the mass modelling of the Matoa fruit. However, Matoa does not have uniformly spherical fruits. Instead, it has a characteristic, thick pericarp and an irregular ellipsoid shape, which differs considerably among varieties (purple vs. red). Normal spherical models do not work well when it comes to estimating the mass of such irregular agricultural products. Thus, this research paper aims to address this gap by: (1) creating a detailed database of physical properties of purple and red Matoa, and (2) creating and testing variety-specific quadratic regression models. These contributions are essential to the design of low-cost, automated grading systems capable of managing the morphological irregularities of the *Sapindaceae* family.

MATERIALS AND METHODS

Materials

Two ripe Matoa fruits (Figure 2) with different varieties (purple and red) were harvested from a Mukah, Sarawak farm. Harvesting of the fruits was at the commercial maturity (ripe) stage. After the harvesting, the fruits were washed in order to remove foreign material, dust, and remnants of floral. A total of 60 samples (N=60) of 30 purple and 30 red fruits were randomly chosen to be analysed in terms of physical properties. Before measuring it, samples were screened to exclude all defects, physical damage, and pest infestation. It is important to note that all the experiments were carried out on the same day when the fruits were picked at room temperature.

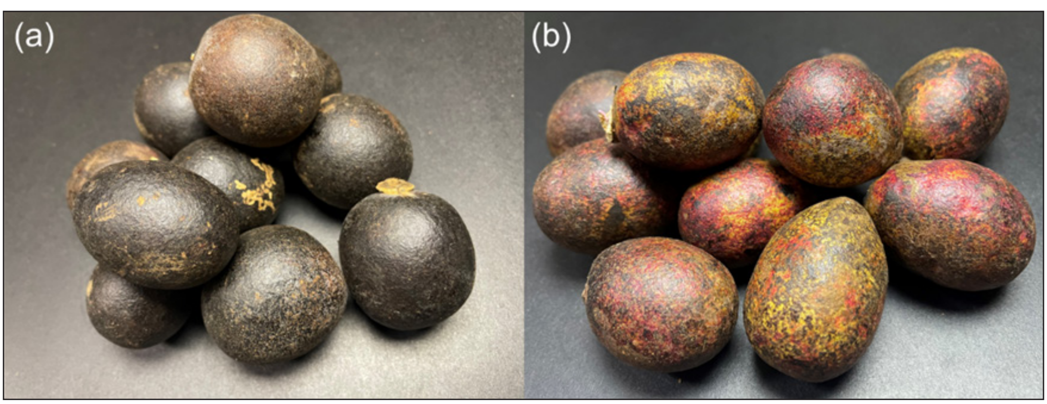

Figure 2. Matoa fruit (*Pometia pinnata*): (a) purple Matoa and (b) red Matoa

Determination of Matoa Fruit Dimension Properties

The test of physical properties was carried out on randomly picked fruits. The palm fruitlets' dimensions, the primary diametre (L), intermediate diametre (W) and minor diametre (T) were taken and recorded on a digital vernier calliper (Mitutoyo, Japan) with a precision of 0.01 mm. The visual observation showed that Matoa fruits are not exactly spherical but assume the shape of an ellipsoid. Therefore, the volume of the fruit was modeled using three geometric approximations (ellipsoid, prolate spheroid, and oblate spheroid) because their geometric shapes are more rigorous mathematical approximations of fruits that do not have equal axes (L, W and T). The physical properties, such as fruit's equivalent mean diametre (D_e), geometric mean diametre (D_g), and arithmetic mean diametre (D_a), were calculated following standard agricultural engineering protocols established by relationships (Mohsenin, 1986), which serve as the fundamental benchmark for characterising biological materials. The Da, Dg, and De were calculated using Equations 1, 2, and 3, respectively.

$$D_a = \frac{(L + W + T)}{3} \quad [1]$$

$$D_g = (L \times W \times T)^{1/3} \quad [2]$$

$$D_e = \left[\frac{[L \times (W \times T)^2]}{4}\right]^{1/3} \quad [3]$$

where D_a denotes the arithmetic mean diametre, D_g represents the geometric mean diametre, D_e portrays the equivalent mean diametre, L stands for the primary diametre (mm), W signifies the intermediate diametre (mm), and T illustrates the minor diametre (mm).

Determination of Matoa Fruit Surface Area

The geometric shapes of the fruitlet s are represented as ellipsoidal and spherical with their corresponding equations as shown below, using which the formula of Surface Area (SA) was calculated as indicated by Equation 4 (Pradhan et al., 2008):

$$SA = \pi {D_g}^2 \quad [4]$$

where SA represents the fruit's SA (mm^2), D_g stands for geometric mean diametre.

The Criteria Projected Area (CPA) of the entire fruit was calculated using the formulae 5, 6, 7, and 8 applied by (Vivek et al., 2018):

$$PA_L = \frac{\pi \times L \times W}{4} \quad [5]$$

$$P_{AW} = \frac{\pi \times W \times W}{4} \quad [6]$$

$$PA_T = \frac{\pi \times T \times W}{4} \quad [7]$$

$$CPA = \frac{P_L + P_W + P_T}{3} \quad [8]$$

where PA_L depicts the projected area perpendicular to the primary diametre (mm^2), PA_W portrays the projected area perpendicular to the intermediate diametre (mm^2), PA_T signifies the projected area perpendicular to the minor diametre (mm^2), and CPA illustrates the criteria projected area (mm^2).

The sphericity ∅ and A_r demonstrate that the fruit's aspect ratio was determined using the following expression Equations 9 and 10, respectively (Goyal et al., 2007; Mohsenin, 1986):

$$\emptyset = \frac{(L \times W \times T)^{1/3}}{L} \quad [9]$$

$$R_a = \frac{W}{L} \quad [10]$$

where ∅ the sphericity (dimensionless) and Ra are the aspect ratios.

Determination of Matoa Fruit Gravimetric Properties

The bulk density of the fruitlets was used to calculate the weight density of the fruits in a 1000 ml cylindrical container by filling it with the fruits, but not compacted and weighing the content using a digital weighing balance (AY120, Shimadzu Corporation, Japan) whose accuracy was set at 0.001 g (Gupta & Das, 1997; Sirisomboon et al., 2007). The density of the bulk was determined using the mass of the fruits and the volume of the container using Equation 11:

$$\rho_b = \frac{m_b}{V_b} \quad [11]$$

where ρ_b demonstrates the fruits' bulk density (kg/m^3), m_b represents the fruitlets' bulk mass (kg), and V_b signifies the container's volume (m^3).

The actual density is calculated as the average weight of the individual fruitlets of the fruits divided by the correct volume as given in Equation (12). The specific weight of fruitlets (AY120, Shimadzu Corporation, Japan) was measured using a digital weighing balance. This meant that the volume of the fruitlets was ascertained using the water displacement method that had been embraced by (Mohsenin, 1986). The water displaced weight was measured, inserted, and used in Equation (12) to calculate the fruitlets' volume. Besides, the volume of an ellipsoid (V_{ellip}), the volume of the prolate spheroid (V_{pro}), and the volume of an oblate spheroid (V_{osp}) were further calculated using Equations 13 – 16 Sanganamoni et al., (2024):

$$V = \frac{m_w}{\rho_w} \quad [12]$$

$$\rho_t = \frac{m_s}{V_s} \quad [13]$$

$$V_{ellip} = \frac{4\pi}{3} \times \left[\frac{a}{2}\right] \times \left[\frac{b}{2}\right] \times \left[\frac{c}{2}\right] \quad [14]$$

$$V_{pro} = \frac{4\pi}{3} \times \left[\frac{a}{2}\right]^2 \times \left[\frac{b}{2}\right] \quad [15]$$

$$V_{osp} = \frac{4\pi}{3} \times \left[\frac{a}{2}\right] \times \left[\frac{b}{2}\right]^2 \quad [16]$$

where V is the volume of individual fruitlets (mm^3), ρ_t represents the fruit's actual density(kg/m^3), m_w demonstrates the water displaced mass (kg), ρ_w signifies the water's density (1000 kg/m^3), V_{ellip} stands for volume of an ellipsoid (mm^3), V_{pro} portrays volume of prolate spheroid (mm^3), and V_{osp} illustrates volume of an oblate spheroid (mm^3).

Porosity, ε, portrays the pores' amount in a bulk material. It is determined using Equation 17 (Mohsenin, 1986):

$$\varepsilon = \left[1 - \frac{\rho_b}{\rho_t}\right] \times 100 \quad [17]$$

where ε represents the porosity, ρ_b stands for the bulk density of fruits (kg/m^3), and ρ_t demonstrates the proper density of fruits (kg/m^3).

Determination of Matoa Fruit Frictional Properties

The static friction coefficients of the fruits were examined on a Mild Steel (MS) and Stainless Steel (SS) surfaces. Thus, the friction angle was calculated utilising a piece of tilting equipment that could be increased by a screw device to alter the tilting angle. An open-ended plastic box (50 mm x 50 mm x 50 mm) was placed horizontally on an adjustable tilting plate and filled with the fruit sample. Hence, the box was lifted slightly to prevent direct contact with the plate surface. Besides, the angle of tilt was measured using a protractor on the side as the plate's inclination was gradually raised by adjusting the screw until the box began to slide down. This was carried out on three different samples. Equation 18 was applied to determine the coefficient of static friction:

$$\mu = \tan\alpha \qquad [18]$$

where μ represents the friction's coefficient, α stands for the angle of tilt (º).

Determination of Matoa Fruit Colour Properties

Colour is one of the main sensory properties, and in many cases, the presence of anthocyanins (Radunić et al., 2015). To measure the colour value of Matoa fruit in other varieties (purple and red), an UltraScan Pro spectrophotometer (D65 HunterLab) was used to determine the colour values of Matoa pericarp. The intensity of colour was indicated by *L*-value (ranging from 0 for darkness to 100 for lightness), *a*-value (from +a for redness to −a for greenness), and *b*-value (from +b for yellowness to −b for blueness) (Wondi et al., 2020). Meanwhile, Chroma (C) and Hue angle (H) were computed from the *L*, a*,* and *b** values employing formulas 19 and 20 (Grover et al., 2024):

$$C = \sqrt{(a*)^2 + (b*)^2} \qquad [19]$$

$$C = \sqrt{(a*)^2 + (b*)^2} \qquad [20]$$

Mass Modelling

The mass of Matoa fruit was predicted based on the calculated physical properties (such as dimensional measurements, volume, and projected area) using five respective model equations outlined in Table 1. Mass modelling was categorised into three approaches: (1) Linear Dimensions, (2) Projected Area, and (3) Calculated Volume:

1. Development of a single-variable regression model for fruit mass referring to the linear dimensions, including D_e, D_g, D_a, thickness (T), width (W), and length (L).
2. Development of a multiple-variable regression model for fruit mass using projected areas, including CPA, projected area perpendicular to minor diameter (PA_T), projected area perpendicular to intermediate diameter (PA_W), projected area perpendicular to primary diametre (PA_L), and SA.
3. Development of a single-variable regression model for fruit mass considering measured ellipsoid volume (V_{ellip}), Oblate spheroid volume (V_{osp}), and Prolate spheroid volume (V_{pro}).

Based on experimental observations, five regression models; linear, quadratic, S-curve, power, and logarithmic, were applied to predict the mass of purple and red variety Matoa fruits. Consequently, the equations for these models are provided in Table 1. In these equations, M represents the mass of the fruit in grams, X denotes the physical parameter used to predict its relationship with mass, and a, b, and c are the curve-fitting constants specific to each model. Thus, the Coefficients of Determination (R^2) value for each model, which approaches 1.00, indicates the best-fit model. Note that a high SEE indicates an unstable dataset model, while a low SEE indicates a reliable model.

Table 1
Mathematical mass models for Matoa fruit

No.	Model	Equations
1	Linear	$M = a + bX$
2	Quadratic	$M = a + bX + cX^2$
3	S-curve	$M = a + (b/X)$
4	Power	$M = aX^b$
5	Logarithmic	$M = a + b \ln(X)$

RESULTS AND DISCUSSION

Physical Properties of Matoa Fruits

Table 2 presents the average, maximum, and minimum values of the physical characteristics of Matoa fruit in different varieties (purple and red varieties). The mean mass values for the purple variety were 42.86 g ± 3.13 for mass (M), 54.22 mm ± 2.64 for primary diameter (L), 45.22 mm ± 0.91 for intermediate diametre (T), and 44.10 mm ± 0.88 for minor diametre (W). For the red variety, the mean values were 17.55 g ± 3.32 for mass, 40.95 mm ± 5.38 for primary diametre, 30.88 mm ± 3.10 for intermediate diametre, and 30.31 mm ± 3.05 for minor diametre. The purple Matoa fruit had higher mass, primary, intermediate, and minor diametre values than the red variety. These dimensional differences resulted in substantially larger arithmetic (D_a = 47.84 mm ± 1.37), geometric (D_g = 47.63 mm ± 1.30), and equivalent diametre (D_e = 47.63 mm ± 1.30) for purple Matoa, whereas the corresponding values for red Matoa ranged between 33.71 and 34.04 mm.

Shape-related parameters further differentiated the two varieties. Purple Matoa exhibited an aspect ratio of 0.88 ± 0.02 and sphericity of 0.85 ± 0.03, indicating a shape closer to spherical. Sphericity, which describes how closely a shape approximates that of a sphere, is ideal when the value is 1.00 (Megat Ahmad Azman et al., 2020; Wondi et al., 2021). Being a Sapindaceae, Matoa has similar morphological features to Lychee (Litchi chinensis) and Longan (Dimocarpus longan). In this case, the value of sphericity is 0.85 (purple) and 0.78 (red), which are similar to those observed with Lychee (0.73–0.76) but not so high as Longan, which is generally more spherical (>0.90) (Jalgaonkar et al., 2017). Nevertheless, the red Matoa has an aspect ratio indicating a more rounded form, unlike the rest of its round relatives. It means that although Longan can be easily placed with the help of rolling mechanisms, red Matoa might need to be placed on the belt sorting to avoid excessive sliding or unbalanced rotations. Actual density and porosity are essential factors in the design of hoppers and in regulating flow rates for fruit processing, grading, conveyance, and packaging equipment. Red Matoa showed a true density of 790 kg/m3 ± 0.06 while the corresponding value for purple Matoa was 660 kg/m3 ± 0.09. Porosity was also slightly higher for red Matoa, indicating a looser packing structure that may facilitate better aeration during storage and transportation (Barbhuiya et al., 2020; Wondi et al., 2021). Porosity is also a valuable characteristic that determines the best fruit storage temperature.

Table 2
Physical properties of Matoa fruit in different varieties (purple and red)

Properties	Variety					
	Purple			Red		
	Min.	**Max.**	**Mean**	**Min.**	**Max.**	**Mean**
M (g)	38.44	47.31	42.86 ± 3.13	13.72	24.66	17.5 ± 3.32
L (mm)	50.42	58.70	54.22 ± 2.64	34.28	53.56	40.95±5.38
W (mm)	43.83	46.63	45.22±0.91	27.54	38.37	30.88±3.10
T (mm)	42.66	45.69	44.10±0.88	27.29	37.71	30.31±3.05
D_a	46.05	50.34	47.84±1.37	29.70	43.21	34.04±3.83
D_g	45.89	50.01	47.63±1.30	29.53	42.63	33.71±3.72
D_e	45.89	50.01	47.63±1.30	29.53	42.63	33.71±3.72
R_a	0.85	0.91	0.88±0.02	0.80	0.86	0.83±0.02
S	0.81	0.89	0.85±0.03	0.74	0.82	0.78±0.02
ρ_t (kg/m^3)	540	800	660±0.09	720	880	790±0.06
ε (%)	33.41	55.32	43.71±7.92	42.36	52.9	46.07±3.95
SA (mm^2)	6615	7858	7133±3.90	2741	5711	3610±8.74
V (mm^3)	55520	79250	66420±0.92	17600	32880	22500±0.50
PA_L (mm^2)	1754	2150	1927±1.27	742	1614	1005±2.47
PA_W, (mm^2)	1509	1708	1607±0.65	596	1156	756±1.61
PA_T, (mm^2)	1469	1674	1568±0.61	590	1137	742±1.58
CPA (mm^2)	1586	1844	1700±0.81	643	1302	834±1.88
V_{ellip}, (mm^3)	50590	65490	56690±0.47	13490	40580	20760±0.78
V_{pro}, (mm^3)	42920	52020	47260±0.28	10840	29070	15570±0.53

Table 2 (*continued*)

Properties	**Variety**					
	Purple			**Red**		
	Min.	**Max.**	**Mean**	**Min.**	**Max.**	**Mean**
V_{osp}, (mm^3)	47380	60630	52940±0.40	12610	36880	19010±0.70
μ (°) MS	10.50	12.30	11.31±0.62	10.80	11.70	11.92±0.65
μ (°) SS	9.82	12.98	11.19 ± 1.31	7.67	8.75	8.09±0.55
*L**	24.04	27.00	25.22 ± 0.96	27.54	30.72	29.01±1.02
*a**	1.47	3.48	2.13±0.61	5.46	15.40	11.40±2.69
*b**	-0.47	2.31	0.52±1.03	2.66	9.75	5.91±2.30
Chroma	1.54	4.18	2.33 ± 0.84	7.86	17.79	13.01±2.80
Hue	-17.73	38.23	8.20 ± 21.22	14.24	46.03	27.57 ± 10.43

Note. Data are expressed as: Mass, M; Major diametre, L; Intermediate diametre, W; Minor diametre, T; Arithmetic mean diametre, D_a; Geometric mean diametre, D_g; Equivalent mean diametre, D_e; Sphericity, S; Aspect ratio, R_a; True density, ρ_t; Porosity, ε; Surface area, SA; Volume, V; Projected area perpendicular to L, PA_L; Projected area perpendicular to W, PA_W; Projected area perpendicular to T, PA_T; Criteria projected area, CPA; Ellipsoid volume, V_{ellip}; Prolate spheroid volume, V_{pro}; Oblate spheroid volume, V_{osp}; Coefficient of friction, μ; MS, Mild steel; SS, Stainless steel

Purple Matoa also recorded substantially higher surface area (7133 mm^2 ± 3.90) and volume (66420 mm^3 ± 0.92). These parameters are particularly important for thermal and mass transfer processes such as drying, cooling, and aeration. Projected area measurements followed similar trends. Purple Matoa showed larger projected areas in all orientations, with mean PA_L, PA_W, PA_T, and CPA values of 1927 mm^2 ± 1.27, 1607 mm^2 ± 0.65, 1568 mm^2 ± 0.61, and 1700 mm^2 ± 0.81, respectively, compared with 1005 mm^2 ± 2.47, 756 mm^2 ± 1.61, 742 mm^2 ± 1.58, and 834 mm^2 ± 1.88 for red Matoa. Among these, CPA was the highest for both varieties, highlighting its relevance in estimating respiration rate and heat and mass transfer during postharvest handling (Mahawar et al., 2019; Megat Ahmad Azman et al., 2020). The mean values for the V_{ellip}, V_{pro} and V_{osp} for purple Matoa were recorded as 56690 mm^3 ± 0.47, 47260 mm^3 ± 0.28, and 52940 mm^3 ± 0.40, respectively. The mean values for red Matoa fruit were as follows: V_{ellip}, 20760 mm^3 ± 0.78; V_{pro}, 15570 mm^3 ± 0.53; and V_{osp}, 19010 mm^3 ± 0.70. The physical properties play a very important role in the design and development of machine vision-based grading systems (Dono et al., 2024; Saikumar et al., 2023). Volume estimates based on ellipsoidal, prolate, and oblate spheroidal models further confirmed the consistently larger size of the purple variety.

The frictional behaviour of Matoa fruits varied with surface material. On mild steel surfaces, the mean friction angles were comparable for purple (11.31° ± 0.62) and red Matoa (11.92° ± 0.65). However, lower friction angles were observed on stainless steel surfaces, particularly for red Matoa (8.09° ± 0.55), indicating reduced resistance to movement and suggesting stainless steel as a more suitable material for smooth conveying applications. Colour parametres (L^*, a^*, and b^*) also revealed distinct varietal differences. Purple Matoa exhibited lower lightness (L^* = 25.22 ± 0.96), chroma (2.33 ± 0.84), and colour intensity, whereas red Matoa showed higher values of L^* (29.01 ± 1.02), a^* (11.40 ± 2.69), b^* (5.91 ± 2.30), chroma (13.01 ± 2.80), and hue angle (27.57° ± 10.43), indicating brighter and more saturated pigmentation. These differences are particularly relevant for machine vision-based grading and automated quality assessment systems.

Mass Modelling

Mass modelling was done on the average dimensions, volumes, weights, SA and projected areas of the various Matoa fruit varieties. Tables 3, 4 and 5 show the summary of the best-performing models that are found, R^2, SEE, F-value and significance level (Sig.) of the predictor of mass of dimension, SA and volume-based model. The selection of the model was largely based on the maximum value of R^2 (nearer to 1.00). Nevertheless, the F-value was used as a secondary measure to evaluate the robustness of the model. The higher the F-value, the higher the signal-to-noise ratio and the greater predictive efficiency. Importantly, the SEE values of Power, S-curve and logarithmic models are on the basis of log-transformed data, and they can not be directly compared to the linear-scale SEE of the Quadratic models. The analysis showed that the quadratic regression model always gave the highest coefficient of determination (R^2) and the lowest Standard Error of Estimate (SEE) on a comparison of linear, S-curve, power, and logarithmic models. This is due to a superior performance, which is a result of the geometric association between the linear dimensions of a fruit and its mass. Volume is intrinsically associated with mass, and it is a three-dimensional property (approximately proportional to L x W x T). Therefore, the correlation between one linear (1D) and mass (3D) is non-linear in nature. This geometric curvature is better represented by the quadratic model ($M = a + bX + cX^2$). Nonetheless, in the case of the Red, more elongated species, which appears more of an ellipsoidal form, the models of logarithms were often more successful at stable volumetric parameters, indicating a different mass distribution of morphological phenomena of volumetric parameters of the spherical purple variety.

Models Based on Dimensions

Table 3 depicts the best-performing mass model that has been determined by a dimension-based method, which includes independent parameters that include: sphericity (S), arithmetic mean diametre (D_a), geometric mean diametre (D_g), minor diametre (W), intermediate diametre (T), and major diametre (L). In addition, the findings showed that the purple and red Matoa varieties are the best fit in the quadratic model. The purple Matoa variety was

Table 3
Mass models of Matoa fruit in different varieties (purple and red) are based on dimension

Independent Parameter	Variety	Best Model	Regression Constant			Statistical Parameters			
			a	b	c	R^2	SEE	Sig.	F-value
L	Purple	Logarithmic	-198.105	60.364	-	0.883	1.134	< 0.05	60.504
	Red	Quadratic	-13.135	0.901	-0.004	0.883	1.287	< 0.05	26.367
W	Purple	Quadratic	-26.892	-9.873	0.034	0.806	1.462	< 0.05	33.230
	Red	Quadratic	-46.593	3.021	-0.030	0.929	0.999	< 0.05	46.127
T	Purple	Quadratic	613.941	-28.648	0.356	0.617	2.195	< 0.05	5.638
	Red	Quadratic	-48.629	3.210	-0.034	0.917	1.081	< 0.05	38.849
D_a	Purple	Quadratic	-559.413	22.886	-0.215	0.962	0.689	< 0.05	89.227
	Red	Quadratic	-31.469	1.990	-0.016	0.911	1.124	< 0.05	35.664
D_g	Purple	Quadratic	-613.483	25.152	-0.239	0.959	0.720	< 0.05	81.546
	Red	Logarithmic	-89.259	30.405	-	0.913	1.039	< 0.05	83.682
S	Purple	Quadratic	717.350	-1502.366	832.450	0.641	2.126	< 0.05	6.241
	Red	Quadratic	719.638	-1697.979	1021.565	0.608	2.355	< 0.05	5.421

Note. Data are expressed as: Major diameter (L); Intermediate diameter (W); Minor diameter (T); Arithmetic mean diameter (D_a); Geometric mean diameter (D_g); Sphericity (S)

well fitted by the quadratic model. D_a and D_g were among the dimensional parameters that provided very precise predictions, with which a single-dimensional predictor can be relied upon to predict the grading. D_a model was the best predictor (Figure 3), with the highest coefficient of determination (R^2=0.962) and F-value (F=89.23, $p < 0.001$) of the purple variety. A residual analysis was done to identify any form of systematic bias. As depicted in Figure 4, the random scatter of standardised residuals around the zero axis confirms homoscedasticity and the absence of any systematic bias, validating the model's reliability for mass grading of the spherical purple fruit. This indicates that the arithmetic average of axes will provide the mass distribution of the spherical purple fruit well. Another model that performed well was the D_g model with an R^2 of 0.959 and an F-value of 81.55. D_g is a theoretically acceptable predictor, although slightly less than D_a, as it explains the geometric product of the three axes. The best-fitting equations for the purple variety are presented in Equations 21 and 22:

$$M = -559.41 + 22.89D_a - 0.22\,{D_a}^2 \qquad [21]$$

$$M = -613.48 + 25.152D_g - 0.24\,{D_g}^2 \qquad [22]$$

For the red Matoa fruit, the linear dimensions specifically intermediate diametre (W) and minor diametre (T) yielded the most accurate predictions among the raw dimensions. The Width (W) quadratic model achieved the highest accuracy with an R^2 of 0.929 (*F = 46.13*). However, a distinct deviation was observed for the mean diametre. The Logarithmic model provided the best fit for the D_a, achieving an R^2 of 0.945 and a remarkably high F-value of 137.09. This reinforces the observation that the elongated red variety scales differently than the spherical purple variety. The best-fitting equations for the red variety are presented in Equations 23 and 24:

$$M = -46.59 + 3.12W - 0.03\,W^2 \qquad [23]$$

$$M = -389.38 + 111.89\ln(\mathrm{D_a}) \qquad [24]$$

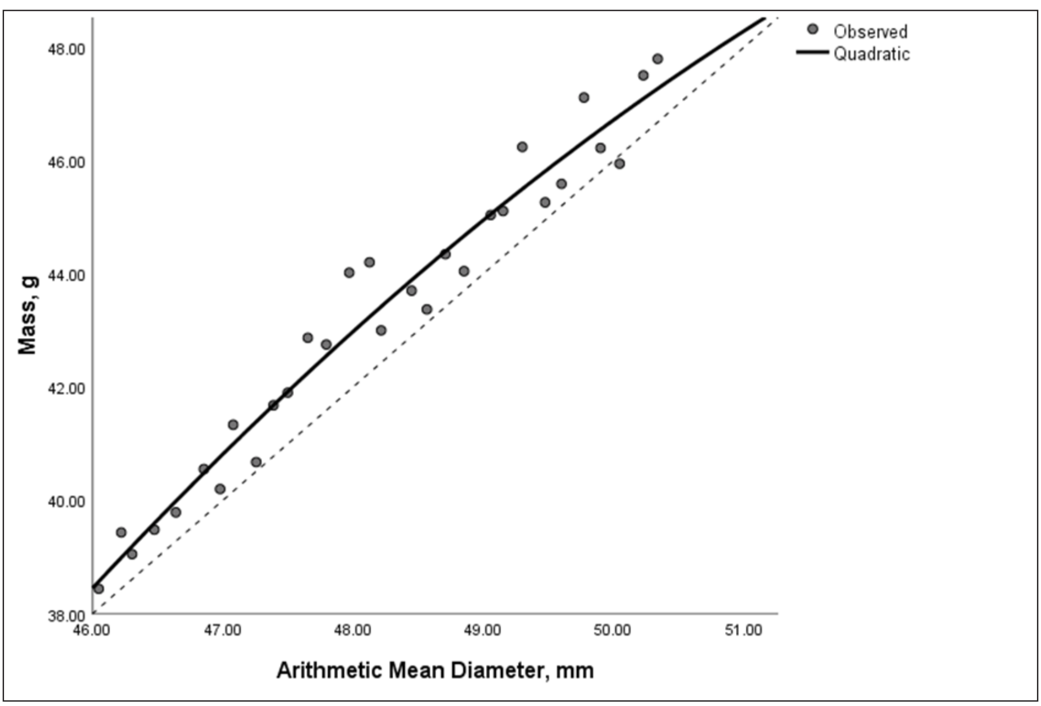

Figure 3. Best-fitting quadratic regression models for purple variety Matoa fruit mass prediction based on Arithmetic Mean Diametre (D_a), showing the highest single-dimensional accuracy (R^2=0.962)

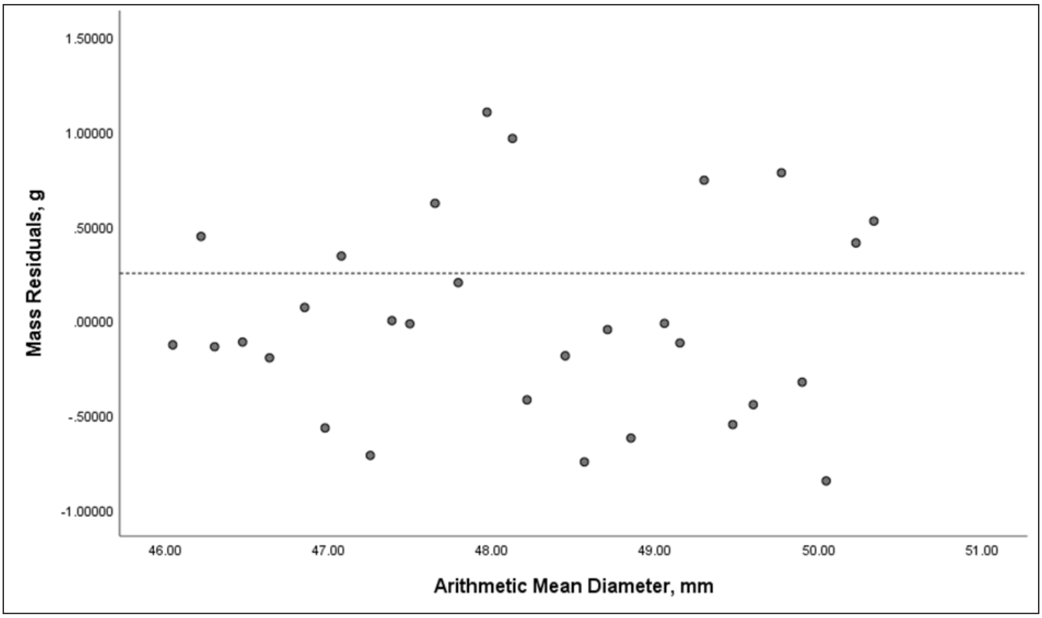

Figure 4. Residual diagnostics for the quadratic mass model of purple variety Matoa based on the Arithmetic Mean Diametre, D_a. The random scatter of the standardised residuals around the zero-line visually confirms constant variance of errors and demonstrates the absence of any systematic bias in the model predictions across the entire range of observed mass values

Model Based on Surface Area

A quadratic model provided the best fit for predicting the mass of Matoa fruit based on Surface Area (SA) parameters (Table 4). The SA-based modelling has been used to predict the mass of both purple and red Matoa fruits using Criteria Projected Area (CPA), PA_T, PA_W, PA_L, and SA. In the purple fruits, the most accurate predictions were obtained by the total Surface Area (SA) and Projected Area (PA_L). The SA model achieved an R^2 of 0.960 and a high F-value of 82.93 ($p < 0.001$). Equally, the PA_L model demonstrated an R^2 of 0.945. Such strong correlations affirm that optical systems that quantify the projected area are capable of estimating mass. This is a better performance ($R^2 = 0.94$) than that shown with Sohiong fruit ($R^2 = 0.88$), presumably because the pericarp of Matoa is smoother and thus more area can be measured in this case than with the rough-skinned fruits. The best parameters, together with the associated model equations, are as follows stated in Equations 25 and 26:

$$M = -163.06 + 0.05SA - 35.16\,SA^2 \quad [25]$$

$$M = -73.69 + 0.097PA_L - 23.9\,{PA_L}^2 \quad [26]$$

On the other hand, the red variety had a high affinity to SA using the Logarithmic models as in Equation 27. The Logarithmic model of SA had an R^2 value of 0.940 and a very significant F-value of 126.3 against the Quadratic model (R^2=0.914). Mechanically, this verifies the fact that the mass distribution of the red variety in relation to the surface area involves a logarithmic trend due to its lower sphericity. However, for lateral projections (PA_W), as in Equation 28, the Quadratic model remained optimal:

$$M = -305.57 + 46.08 \, ln\,(SA) \quad [27]$$

$$M = -10.42 + 0.05PA_W - 22.91\, {PA_W}^2 \quad [28]$$

Models Based on Volume

Table 5 shows the best-performing model parameters determined by use of a volume model, which took into account Oblate (V_{osp}), Prolate (V_{pro}) and Ellipsoid (V_{ellip}) volumes in estimating the mass of the purple and red Matoa fruits. These findings indicate that a quadratic model best fits the mass of the purple fruit, given the Vellip, with the highest R^2 of 0.960. This is consistent with the physical fact that in spherical fruits, the distribution of densities is relatively constant and hence volume is an almost ideal predictor of mass as indicated in Equation 29:

$$M = -67.28 + 0.003V_{ellip} - 30.32\, {V_{ellip}}^2 \quad [29]$$

In agreement with the area models, the red variety was found to respond to the Logarithmic model in predicting mass using V_{ellip} with a higher R^2 of 0.913 with a much higher F-value (F=83.9) than the Quadratic model. But in the case of V_{osp}, the Quadratic model fit best (R^2=0.914). This finding corresponds to the results of Sumit Sudhir et al. (2019) with dried *Terminalia chebula*, who found that, depending on the aspect ratio of the fruit, the plotted geometric approximation (Oblate vs. Ellipsoid) would dramatically change their best-fitting regression curve. Equation 30, the quadratic model, is as follows:

$$M = -86.61 + 0.004V_{osp} - 39.14\, {V_{osp}}^2 \quad [30]$$

CONCLUSION

This study successfully characterised the physical parameters of various Matoa fruit varieties and established their robust association with fruit mass. The study revealed that purple and red Matoa varieties are highly differentiated in terms of size, mass, and shape, where the purple one is always more massive and spherical. The mass modelling that followed identified that the quadratic regression model is the best mathematical tool that

Table 4
Mass models of Matoa fruit in different varieties (purple and red) based on area

Independent Parameter	Variety	Best Model	Regression Constant			Statistical Parameters			
			a	b	c	R^2	SEE	Sig.	F-value
SA	Purple	Quadratic	-163.060	0.050	-35.16	0.960	0.714	< 0.05	82.931
	Red	Logarithmic	-106.669	15.203	-	0.913	1.038	< 0.05	83.888
P_{AL}	Purple	Quadratic	-73.686	0.097	-23.90	0.945	0.835	< 0.05	59.679
	Red	Logarithmic	-82.285	14.490	-	0.908	1.066	< 0.05	79.065
P_{AW}	Purple	Quadratic	163.395	-0.194	7.394×10^{-5}	0.813	1.534	< 0.05	15.212
	Red	Quadratic	-10.420	0.051	-22.91	0.930	0.996	< 0.05	46.416
P_{AT}	Purple	Quadratic	111.634	-0.132	5.598×10^{-5}	0.745	1.790	< 0.05	10.244
	Red	Quadratic	-10.780	0.053	-24.13	0.925	1.028	< 0.05	43.359
CPA	Purple	Quadratic	-149.207	0.189	-49.49	0.923	0.983	< 0.05	42.110
	Red	Quadratic	-7.686	0.041	-17.53	0.921	1.054	< 0.05	41.015

Note. Data are expressed as: Surface area (SA); Volume (V); Projected area perpendicular to L (PA_L); Projected area perpendicular to W (PA_W); Projected area perpendicular to T (PA_T); Criteria projected area (CPA)

Table 5
Mass models of Matoa fruit in different varieties (purple and red) based on volume

Independent Parameter	Variety	Best Model	Regression Constant			Statistical Parameters			
			a	b	c	R^2	SEE	Sig.	F-value
V_{ellip}	Purple	Quadratic	-67.278	0.003	-30.320	0.960	0.709	< 0.05	84.042
	Red	Logarithmic	-82.707	10.136	-	0.913	1.038	< 0.05	83.889
V_{pro}	Purple	Quadratic	53.926	-0.001	-33.830	0.776	1.678	< 0.05	12.135
	Red	Quadratic	-0.115	0.002	-28.670	0.927	1.013	< 0.05	44.729
V_{osp}	Purple	Quadratic	-86.606	0.004	-39.140	0.934	0.911	< 0.05	49.567
	Red	Quadratic	2.096	0.001	-17.910	0.914	1.103	< 0.05	37.187

Note. Data are expressed as: Ellipsoid volume (V_{ellip}); Prolate spheroid volume (V_{pro}); Oblate spheroid volume (V_{osp})

can be used to predict fruit mass of all the tested physical characteristics. The implication of these results in practical terms is that the design of automated grading systems cannot be neglected as the correlation between projected area and mass is very high which guarantees that low-cost machine vision systems can be calibrated to substitute slower and more expensive load-cell-based weighing systems providing a feasible pathway to high-speed, non-contact grading that will have a strong impact on economic efficiency and labour intensity. In addition, the calculated coefficients of friction and the data of sphericity offer invaluable information in dealing with the design, namely the use of stainless steel surfaces to reduce damage, and it would require a particular conveyor design to deal with the more ellipsoidal red one due to its rolling instability. The resulting quadratic models with fruit dimension and approximated volume as the measure of mass prediction have been suggested to be adopted in designing and optimising the post-harvesting machinery to be used in the handling, cleaning, conveying, and storage of Matoa fruit. The scalability and robustness of these quadratic models in a continuous, high-speed industrial sorting environment are therefore worth future research to prove their validity.

ACKNOWLEDGEMENT

This work was supported by the Universiti Teknologi MARA (UiTM) through the Excellence Research Fund (DKCM), Reference No: 600-TNCPI 5/3/DDN (13) (003/2024).

REFERENCES

Afiqah, N., Abdul, H., Shamsudin, R., & Ariffin, S. H. (2024). Physical properties of full-ripe dabai (*canarium odontophyllum miq. variety song*) at different fractions. *Pertanika Journal of Science and Technology*, *32*(2), 725-739. https://doi.org/https://doi.org/10.47836/pjst.32.2.13

Ahemen, S. A., & Raji, A. O. (2017). Moisture-dependent physical properties of Tacca involucrata tubers. *Journal of Food Process Engineering*, 1-8. https://doi.org/10.1111/jfpe.12541

Barbhuiya, R. I., Nath, D., Singh, S. K., & Dwivedi, M. (2020). Mass modelling of indian coffee plum (*Flacourtia Jangomas*) fruit with its physicochemical properties. *International Journal of Fruit Science*, *20*(3), 1-24. https://doi.org/10.1080/15538362.2020.1775161

Bhushan, B., Manoj Kumar, M., Kirti, J., Vijay, S. M., & Dattatreya, M. K. (2022). Mass modelling of guava (*cv. Allahabad safeda*) fruit with selected dimensional attributes: Regression analysis approach. *Journal of Food Process Engineering*, *45*(3), 1-10. https://doi.org/https://doi.org/10.1111/jfpe.13978

Birania, S., Attkan, A. K., Kumar, S., Kumar, N., & Singh, V. K. (2022). Mass modelling of strawberry (Fragaria Ananasa) based on selected physical attributes. *Journal of Food Process Engineering*, *February*, 1-12. https://doi.org/10.1111/jfpe.14023

Chandegara, V. K., & Varshney, A. K. (2014). Design and development of leaf splitting unit for aloe vera gel expulsion machine. *Journal of Food Process Engineering*, *37*(4), 427-437. https://doi.org/10.1111/jfpe.12098

Chapagain, B. P., Saharan, V., & Wiesman, Z. (2008). Larvicidal activity of saponins from Balanites aegyptiaca callus against Aedes aegypti mosquito. *Bioresource Technology*, *99*(5), 1165-1168. https://doi.org/10.1016/j.biortech.2007.02.023

Dono, F. X., Baatuuwie, B. N., Abagale, F. K., & Borgen, P. (2024). Application of computer vision and machine learning in morphological characterisation of Adansonia digitata fruits. *Smart Agricultural Technology*, *9*(June), 1-11. https://doi.org/10.1016/j.atech.2024.100528

Faustina, F. C., & Santoso, F. (2017). Extraction of fruit peels of *Pometia pinnata* and its antioxidant and antimicrobial activities. *Jurnal Penelitian Pascapanen Pertanian*, *11*(2), 80-88. https://doi.org/10.21082/jpasca.v11n2.2014.80-88

Ghazzawi, H. A., Hussain, M. A., Raziq, K. M., Alsendi, K. K., Alaamer, R. O., Jaradat, M., Alobaidi, S., Al Aqili, R., Trabelsi, K., & Jahrami, H. (2023). Exploring the relationship between micronutrients and athletic performance: A comprehensive scientific systematic review of theliterature in sports medicine. *Sports*, *11*(6). https://doi.org/10.3390/sports11060109

Goyal, R. K., Kingsly, A. R. P., Kumar, P., & Walia, H. (2007). Physical and mechanical properties of aonla fruits. *Journal of Food Engineering*, *82*(4), 595-599. https://doi.org/10.1016/j.jfoodeng.2007.03.019

Grover, R., Kumar, A., & Kumar, S. (2024). Physical characterisation and mass modelling of Wood apple (Aegel marmelos L.). *Food Physics*, *1*(May), 100013. https://doi.org/10.1016/j.foodp.2024.100013

Gupta, R. K., & Das, S. K. (1997). Physical properties of sunflower seeds. *Journal of Agricultural and Engineering Research*, *66*(1), 1-8. https://doi.org/10.1006/jaer.1996.0111

Jalgaonkar, K., Mahawar, M. K., Bibwe, B., Dukare, A., Kannaujia, P., & Bhushan, B. (2017). Moisture dependent physical properties of Litchi seeds (Litchi chinensis). *Food & Nutrition Journal*, *5*(6). https://doi.org/10.29011/2575-7091.100048

Jomova, K., Raptova, R., Alomar, S. Y., Alwasel, S. H., Nepovimova, E., Kuca, K., & Valko, M. (2023). Reactive oxygen species, toxicity, oxidative stress, and antioxidants: chronic diseases and aging. *Archives of Toxicology*, *97*(10), 2499-2574. https://doi.org/10.1007/s00204-023-03562-9

Kamble, M. G., Singh, A., Mishra, V., Meghwal, M., & Prabhakar, P. K. (2021). Mass and surface modelling of green plantain banana fruit based on physical characteristics. *Computers and Electronics in Agriculture*, *186*, Article 106194. https://doi.org/10.1016/j.compag.2021.106194

Lorestani, A. N., Jaliliantabar, F., & Gholami, R. (2012). Mass modelling of caper (Capparis spinosa) with some engineering properties. *Quality Assurance and Safety of Crops & Foods*, *4*, 38-42. https://doi.org/10.1111/qas.12004

Mahawar, M. K., Bibwe, B., Jalgaonkar, K., & Ghodki, B. M. (2019). Mass modeling of kinnow mandarin based on some physical attributes. *Journal of Food Process Engineering*, *42*(5), 1-11. https://doi.org/10.1111/jfpe.13079

Megat Ahmad Azman, P. N., Shamsudin, R., Che Man, H., & Ya'acob, M. E. (2020). Some Physical Properties and Mass Modelling of Pepper Berries (Piper nigrum L.), Variety Kuching, at Different Maturity Levels. *Processes*, *6*(1314), 1-15. https://doi.org/10.3390/pr8101314

Mohammad, F. V., Noorwala, M., Ahmad, V. U., Zahoor, A., & Lajis, N. H. J. (2012). A new monodesmosidic triterpenoid saponin from the leaves of *Pometia pinnata*. *Natural Product Communications*, *7*(11), 1423-1426. https://doi.org/10.1177/1934578x1200701105

Mohsenin, N. N. (1986). *Physical Properties of Agricultural Materials and Food Products* (1st ed.). Gordon and Breach Science Publishers.

Murakonda, S., Patel, G., & Dwivedi, M. (2022). Characterisation of engineering properties and modelling mass and fruit fraction of wood apple (Limonia acidissima) fruit for post-harvest processing. *Journal of the Saudi Society of Agricultural Sciences*, *21*(4), 267-277. https://doi.org/10.1016/j.jssas.2021.09.005

Pandiselvam, R., Manikantan, M. R., Balasubramanian, D., Beegum, P. P. S., Mathew, A. C., Ramesh, S. V., Hebbar, K. B., & Niral, V. (2019). Mechanical properties of tender coconut (Cocos nucifera L.): Implications for the design of processing machineries. *Journal of Food Process Engineering*, 1-8. https://doi.org/10.1111/jfpe.13349

Pradhan, R. C., Naik, S. N., Bhatnagar, N., & Vijay, V. K. (2008). Moisture-dependent physical properties of jatropha fruit. *Industrial Crops & Products*, *29*, 341-347. https://doi.org/10.1016/j.indcrop.2008.07.002

Radunić, M., Jukić Špika, M., Goreta Ban, S., Gadže, J., Díaz-Pérez, J. C., & Maclean, D. (2015). Physical and chemical properties of pomegranate fruit accessions from Croatia. *Food Chemistry*, *177*, 53-60. https://doi.org/10.1016/j.foodchem.2014.12.102

Saikumar, A., Nickhil, C., & Badwaik, L. S. (2023). Physicochemical characterization of elephant apple (Dillenia indica L.) fruit and its mass and volume modelling using computer vision. *Scientia Horticulturae*, *314*, Article 111947. https://doi.org/10.1016/j.scienta.2023.111947

Sanganamoni, S., Kancherla, S., Pedapati, A., Akki, S., & Patel, J. (2024). Physical characterisation and development of mathematical models for predicting mass and area of oil palm fruits. *Journal of Food Process Engineering*, *47*(1), 1-24. https://doi.org/10.1111/jfpe.14512

Sauriasari, R., Azizah, N., & Basah, K. (2017). Tyrosinase inhibition, 2,2-diphenyl-1-picrylhydrazyl radical scavenging activity, and phytochemical screening of fractions and ethanol extract from leaves and stem bark of Matoa (*Pometia pinnata*). *Asian Journal of Pharmaceutical and Clinical Research*, *10*(Special Issue), 85-89. https://doi.org/10.22159/ajpcr.2017.v10s5.23105

Sholiha, F. U., Yuniastuti, E., & Hartati, S. (2024). The matK gene analysis in five types of Matoa (*Pometia pinnata J. R. Forst. & G. Forst*) based on the pericarp colour. *Journal of Applied Biology & Biotechnology*, *12*(3), 54-58. https://doi.org/10.7324/JABB.2024.167495

Sirisomboon, P., Kitchaiya, P., Pholpho, T., & Mahuttanyavanitch, W. (2007). Physical and mechanical properties of Jatropha curcas L. fruits, nuts and kernels. *Biosystems Engineering*, *97*, 201-207. https://doi.org/10.1016/j.biosystemseng.2007.02.011

Sumit Sudhir, P., Rama Chandra, P., & Sabyasachi, M. (2019). Physical characterisation and mass modelling of dried Terminalia chebula fruit. *Journal of Food Process Engineering*, *December 2018*, 1-10. https://doi.org/10.1111/jfpe.12992

Viana de Araujo, M. E., Guimarães Barbosa, E., Oliveira, A. C. L., Milagres, R. S., Carvalho Pinto, F. de A., & Corrêa, P. C. (2020). Physical properties of yellow passion fruit seeds *(Passiflora edulis)* during the drying process. *Scientia Horticulturae*, *261*, Article 109032. https://doi.org/10.1016/j.scienta.2019.109032

Vivek, K., Mishra, S., & Chandra, R. (2018). Physicochemical characterisation and mass modelling of Sohiong (Prunus nepalensis L.) fruit. *Journal of Food Measurement and Characterization*, *12*, 923-936. https://doi.org/10.1007/s11694-017-9708-x

Wahedi, J. A., Vincent, V. M., Pukuma, S. M., Bawa, I. S., Agboola, O. O., Aju-Ahmeh, C. O., Filgona, J., & Olowoyo, J. O. (2024). Phytochemical screening and larvicidal activities of Cymbopogon citratus and Annona senegalensis against Culex quinquefasciatus. *Scientific African*, *23*(May 2022), e02057. https://doi.org/10.1016/j.sciaf.2024.e02057

Warraich, U. e. A., Hussain, F., & Kayani, H. U. R. (2020). Aging - Oxidative stress, antioxidants and computational modelling. *Heliyon*, *6*(5), e04107. https://doi.org/10.1016/j.heliyon.2020.e04107

Wondi, M. H., Haris, N. I. N., Shamsudin, R., Yunus, R., Mohd Ali, M., & Iswardi, A. H. (2024). Development and testing of an oil palm (Elaeis guineensis Jacq.) fruit digester process for kernel free in crude palm oil production. *Industrial Crops & Products*, *208,* Article 117755. https://doi.org/10.1016/j.indcrop.2023.117755

Wondi, M. H., Johar, N., Haris, N. I. N., Manaf, S. R., Sulaiman, M. N., Mohd Ali, M., Talip, M. S. A., Kadir, A. R. A., & Fikry, M. (2025). Borneo's Indigenous Fruits as Natural Sources for Nano-Coating Applications: Nutritional and Antioxidant Insights. *Journal of Advanced Research in Micro and Nano Engineering*, *42*(1), 151-176.

Wondi, M. H., Shamsudin, R., Yunus, R., Alsultan, G. A., & Iswardi, A. H. (2020). Centrifugal separation-assisted and extraction of crude palm oil from separated mesocarp fiber: Central composite design optimisation. *Journal of Food Process Engineering*, *43*(7). https://doi.org/10.1111/jfpe.13426

Wondi, M. H., Shamsudin, R., Yunus, R., Baharudin, M. S., Arnan, M. Z., & Rahman, A. F. A. (2021). Physical and mechanical properties of sterilised oil palm fruits at different component. *AMA, Agricultural Mechanization in Asia, Africa and Latin America*, *52*(3), 3985-a3997.

Wondi, M. H., Shamsudin, R., Yunus, R., Mohd Ali, M., & Haris, N. I. N. (2023). Design of a separator machine for oil palm fruit mesocarp and nut using computer-aided design and linear finite element analysis. *Journal of Food Process Engineering*, Article e14457. https://doi.org/10.1111/jfpe.14457